



Daily climate data reveal stronger climate-growth relationships for an extended European tree-ring network

Jernej Jevšenak

Slovenian Forestry Institute, Department of Forest Yield and Silviculture, Večna Pot 2, 1000, Ljubljana, Slovenia

ARTICLE INFO

Article history:

Received 21 May 2019

Received in revised form

5 August 2019

Accepted 5 August 2019

Available online xxx

Keywords:

Tree rings

Dendroclimatology

Tree-ring network

Daily climate data

Climate-growth relationships

dendroTools

ABSTRACT

An extended European tree-ring network was compiled from various sources of tree-ring data from Europe, northern Africa and western Asia. A total of 1860 tree-ring chronologies were used to compare correlation coefficients calculated with aggregated day-wise and month-wise mean temperature, sums of precipitation and standardised precipitation-evapotranspiration index (SPEI). For the daily approach, climate data were aggregated over periods ranging from 21 to 365 days. Absolute correlations calculated with day-wise aggregated climate data were on average higher by 0.060 (temperature data), 0.076 (precipitation data) and 0.075 (SPEI data). Bootstrapped correlations are computationally expensive and were therefore calculated on a 69.4% subset of the data. Bootstrapped correlations indicated statistically significant differences between the daily and monthly approach in approximately 1% of examples. A comparison of time windows used for calculations of correlations revealed slightly later onset and earlier ending day of the year for the daily approach, while the largest differences between the two approaches arise from window lengths: Correlations calculated with day-wise aggregated climate data were calculated using fewer days than the monthly approach. Differences in the onset and ending dates of periods for the daily and monthly approaches were greater for precipitation and SPEI data than for temperature data.

© 2019 Elsevier Ltd. All rights reserved.

1. Introduction

In dendroclimatology, various tree-ring proxies are usually compared to gridded or observed station climate data with monthly resolution to analyse climate-growth relationships (Cook and Kairiukstis, 1992). Monthly climate data are more easily accessible, available for most land territories and have longer time spans than daily data, but at the cost of accuracy, particularly when dealing with precipitation data (Hofstra et al., 2009; Yin et al., 2015). All monthly data, whether they are gridded or from station observations, are derived from daily climate station observations, which are the raw climate products, and then aggregated into monthly datasets. In addition to the many daily observations available from the KNMI Climate Explorer (<https://climexp.knmi.nl/start.cgi>), various reforecast project collaborations have resulted in high quality gridded daily data, such as E-OBS gridded daily datasets for Europe (Corney et al., 2018), Berkeley Earth temperature datasets (<http://berkeleyearth.org>) and various datasets provided

by the National Oceanic and Atmospheric Administration of the United States (<https://www.esrl.noaa.gov/psd/data/gridded/tables/daily.html>).

Daily climate data is well integrated into various process-based models, such as the VS model (Anchukaitis et al., 2006; Shishov et al., 2016) and MAIDENiso (Danis et al., 2012). Some previous dendroclimatological studies have used daily climate data. Land et al. (2017) reported increasing correlations between ring widths and precipitation if heavy precipitation events are excluded from the precipitation data. Their study showed that the annual radial growth of oak trees is mainly affected by daily precipitation sums of less than 10 mm. Schönbein et al. (2015) reconstructed summer precipitation based on subfossil oak tree-ring data and daily precipitation records from southern Germany, while Pritzkow et al. (2016) combined the earlywood vessel area of *Quercus robur* and daily temperature data from northern Poland to reconstruct minimum winter temperatures back to 1810. Climate-growth relationships using daily climate data have been calculated by various authors (e.g. Castagneri et al., 2015; Liang et al., 2013; Sanders et al., 2014; Sun and Liu, 2016). One of the first software programs for dendroclimatological studies based on daily climate data was

E-mail address: jernej.jevsenak@gozdis.si.

CLIMTREG, provided by Beck et al. (2013), while Jevšenak and Levanič (2018) recently presented the dendroTools R package, which is designed for the R environment (R Core Team, 2019) and provides various options for analysis of climate-growth relationships on daily and monthly scales.

Combining tree-ring networks with gridded climate data can provide comprehensive spatio-temporal information related to tree growth and climate sensitivity. Compiled large-scale tree-ring networks have already been used for various purposes, e.g. to analyse climate-growth associations for northern hemisphere tree-ring width records (St. George, 2014); to evaluate the climate sensitivity of model-based forest productivity estimates (Babst et al., 2013); to identify climatic drivers of global tree growth (Babst et al., 2019); to characterise relationships between climate, reproduction and growth (Hackett-Pain et al., 2018); to simulate radial tree growth with the VS-Lite model on a global scale (Breitenmoser et al., 2014); to assess global tree-mortality (Cailleret et al., 2017); and to quantify the drought effect on tree growth as a measure of vitality (Bhuyan et al., 2017). Zhao et al. (2019) analysed representatives and biases of tree-ring records in the Global Tree-Ring Databank (ITRDB), identified priority sampling areas and corrected identified issues, while Babst et al. (2018) discussed challenges and opportunities related to tree-ring networks. No tree-ring network has so far been used to analyse climate-growth relationships for daily data and to compare daily and monthly climate-growth relationships. To do so, an extended European tree-ring network was established using freely available data from various sources and combining these data with gridded daily climate data, i.e. E-OBS daily data on a 0.1-degree regular grid.

In this study, I compare climate-growth correlations calculated from aggregated daily and monthly data of mean temperature, sums of precipitation and standardised precipitation-evapotranspiration indices (SPEI). Climate data with daily resolution enable greater flexibility in the analysis of climate-growth relationships and provide higher explained variance in calibration models for climate reconstructions. In areas where the time period related to the climate signal starts/ends near the 15th day of the month, a daily approach should provide significantly greater differences between correlations calculated from day-wise and month-wise aggregated climate data. An important benefit of using a daily approach is the possibility to study changes in time windows over time. While the temporal stability of monthly data usually enables the study of only the changes in correlation coefficients over time, a daily approach enables the study of changes in temporal windows over time as well. Hypothetically, this information could be used to model the divergence of climate-growth relationships (Loehle, 2009) and changes in growing season patterns (Linderholm, 2006). Finally, studying climate growth correlations using day-wise aggregated climate data could improve our understanding of the climate signal in tree rings and enable us to more accurately predict future growth under different climate scenarios. The goal of this study is to highlight the advantages of using daily rather than monthly data and, at the same time, expose possible caveats related to the daily approach.

The paper is structured as follows: in section 3.1 I give a general description of the extended European tree-ring network, while correlations calculated with day-wise and month-wise aggregated climate data are compared in sections 3.2 and 3.3. The time periods related to the calculated correlation coefficients for the daily and monthly approach are compared in section 3.4. Finally, in section 3.5 the potential applications and future extensions of the daily approach are discussed. In the conclusions the main results are summarised, and possible caveats of the daily approach are discussed.

2. Materials and methods

2.1. Tree-ring network

For the purposes of this study, I compiled a continental-scale tree-ring network consisting of freely available data from various online sources. A cleaned and corrected version of the International Tree Ring Data Bank (Grissino-Mayer and Fritts, 1997), i.e. rITRDB, which was presented by Zhao et al. (2019) and is available via the web repositories of the National Climatic Data Center (<https://www.ncdc.noaa.gov/paleo/study/25570>), was used as the primary source. This dataset consists of 8326 individual files in Tucson format, containing information on various tree-ring parameters. Firstly, rITRDB was updated with 16 additional rwl files from Europe, which were recently added to the International Tree Ring Data Bank. These data are marked "ITRDB_2019" in Supplementary Table S1, while the files available in rITRDB are marked "rITRDB". All files were filtered to keep only those that correspond to the extent of the ensemble version of the E-OBS temperature and precipitation datasets (Cornes et al., 2018). E-OBS datasets cover 25°W to 45°E longitude and 25°N to 71.5°N latitude on a 0.1-degree regular grid (see below for a more detailed description of the E-OBS datasets). Three additional filters were applied to available rwl files: all had to have at least 10 trees within the site, rbar greater than 0.10 and cover at least 30 years in the period 1950–2018, which is the time span of the E-OBS dataset. After filtering these data, I added three additional datasets from the information system PANGAEA (<https://www.pangaea.de/>). One dataset, presented by Tejedor et al. (2017), consists of individual measurements of conifers from the Iberian Peninsula, while two datasets (Sánchez-Salguero et al., 2017, 2018) are available as already developed and standardised tree-ring width chronologies. These files are marked "PANGAEA" in the source column of Supplementary Table S1. Next, 521 standardised ring-width chronologies provided by Babst et al. (2013) as supplementary material were added. Finally, 43 isotope chronologies, available via the repository of freely available data from the BACI H2020 project (<https://www.bgc-jena.mpg.de/geodb/projects/Data.php>), were added. The final network of tree-ring data consisted of 1860 chronologies (Fig. 1).

All files that were available as raw data, i.e. data from rITRDB, ITRDB and some of the PANGAEA files, were detrended using a spline with a 50% frequency cutoff response at 32 years. For detrending, I used the *detrend()* function from the *dpIR* R package (Bunn, 2008). Detrended measurements were averaged to create a single composite series describing site chronology. Chronologies from PANGAEA, Babst et al. (2013) and isotope chronologies from the BACI repository were available as already developed and standardised series and were used as such. Babst et al. (2013) used the same detrending method as in our study, while chronologies from PANGAEA were standardised using negative exponential or linear functions (Sánchez-Salguero et al., 2018) and negative exponential or linear functions and 30-year-long splines (Sánchez-Salguero et al., 2017). For a description of the final database, see section 3.1; the complete meta-data is available in Supplementary Table S1.

2.2. E-OBS daily climate data and SPEI calculation

To create climate variables, the daily mean, minimum and maximum air temperature and sums of precipitation data were downloaded as netCDF files from http://surfobs.climate.copernicus.eu/dataaccess/access_eobs.php. The E-OBS version 19.0e on a 0.1-degree regular grid was used, which was released in March 2019 and covers the time span from January 1st, 1950 to December 31st, 2018. Using the *knnLookup()* function from the *SearchTrees* R

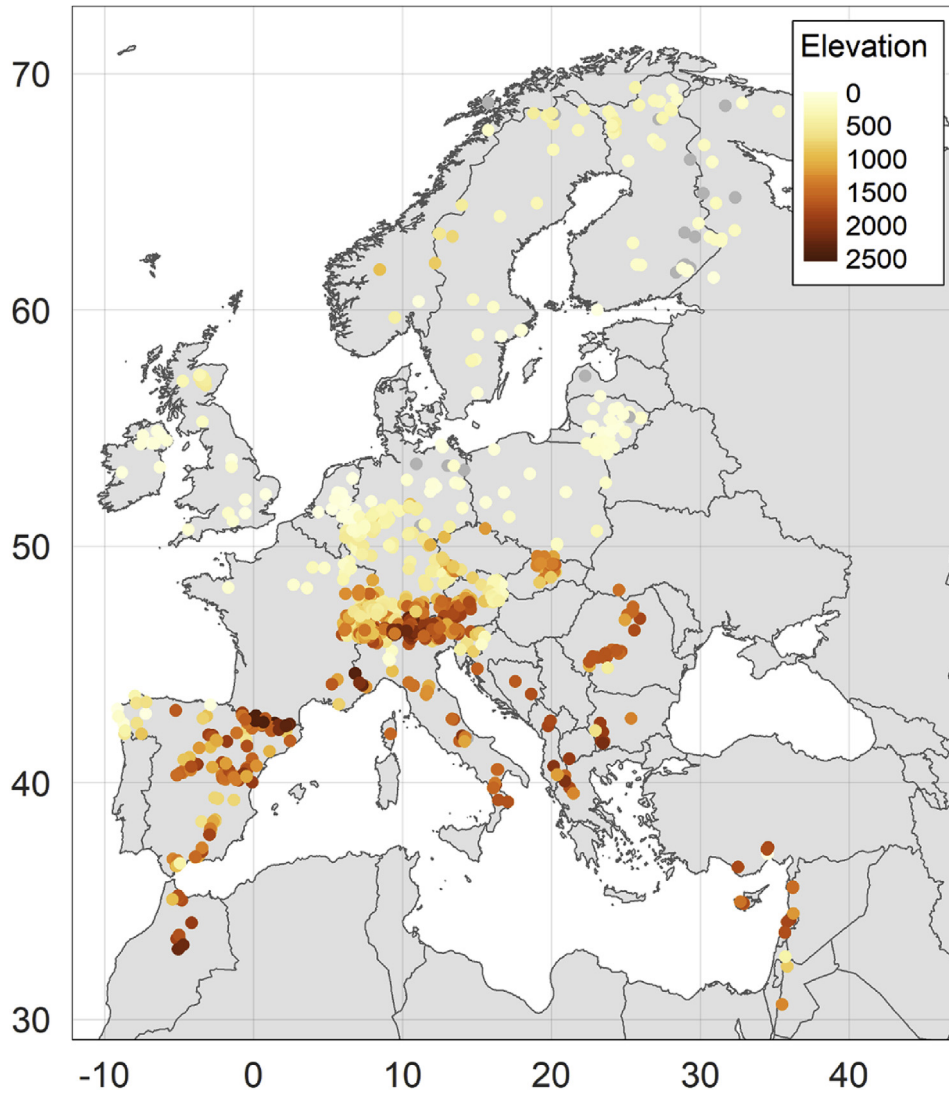


Fig. 1. Locations of analysed chronologies with respective elevation. Missing elevations are marked in grey.

package (Becker, 2012), the closest grid point was located in the E-OBS dataset for each individual site, and climate data were extracted. To study climate growth relationships on daily and monthly scales, mean temperature and sums of precipitation data were used. In addition, downloaded minimum and maximum air temperature data were used to calculate daily and monthly SPEI series (Beguería and Vicente-Serrano, 2017; Vicente-Serrano et al., 2010).

SPEI combines precipitation data and potential evapotranspiration (PET) data. To calculate PET , the Hargreaves-Samani method (Hargreaves and Samani, 1985) was used (Eq. (1)), where T_{mean} is mean daily air temperature, T_{max} is maximum daily air temperature, T_{min} is minimum daily air temperature and R_a is net radiation at the surface (MJm^{-2}/day).

$$PET = 0.0023 (T_{mean} + 17.8) \sqrt{T_{max} - T_{min}} R_a. \quad (1)$$

The R_a for each location and day was estimated from the solar constant and solar declination. A more detailed procedure is described by Wang et al. (2015). Next, the climatic water deficit (D) was calculated for each day (i) as the difference between the daily sum of precipitation (P) and daily PET (Eq. (2)). The calculated D_i values were then aggregated at different daily and monthly time

scales into a log-logistic probability distribution to obtain the SPEI index series, following the same procedure used in the SPEI R package (Vicente-Serrano et al., 2010).

$$D_i = P_i - PET_i \quad (2)$$

2.3. Analysis of daily and monthly climate-growth relationships

Climate-growth relationships for day-wise and month-wise aggregated data were analysed for all chronologies in the final tree-ring network for mean temperatures, sum of precipitation and SPEI. For daily data, the *daily_response()* function from the dendroTools R package (Jevšenak and Levanič, 2018) was used. The *daily_response()* function works by sliding a moving window through daily climate data and calculating correlation coefficients between aggregated daily climate data and the selected tree-ring chronology. With the *daily_response()* function, all correlation coefficients for time windows between 21 and 365 days were calculated. The analysis started with day of year (DOY) 1 and finished with DOY 365. To exclude ecologically impossible effects, e.g. the effect of individual days and very short intervals on annual tree-

ring parameters, the shortest time window considered was 21 days. Therefore, to calculate the first day-wise aggregated correlation coefficient, climate variables were aggregated from DOY 1 to DOY 21, to calculate the second correlation coefficient, climate variables were aggregated from DOY 2 to DOY 22, etc. The last correlation coefficient was calculated using a window size of 365 days, where climate variables were aggregated from DOY 1 to DOY 365. Using this approach, for each chronology and climate variable, the number of calculated correlation coefficients sums to 59 685. The pros and cons of this approach and possible calculations of spurious correlations are discussed later in the conclusions.

Daily datasets were next aggregated into monthly datasets and used in the *monthly_response()* function of the *dendroTools* R package. This function resembles the idea of *daily_response()*: it calculates all possible correlation coefficients between the selected tree-ring chronology and aggregated monthly climate data. All correlation coefficients are therefore calculated for individual months, starting with January, as well as combinations of consecutive months, starting with two consecutive months and finishing with twelve consecutive months. For the monthly approach, the number of calculated correlations between each climate variable and tree-ring chronology is 78. For the daily and monthly approach, the correlation coefficients were calculated using the Pearson method.

After the calculation of all correlation coefficients with *daily_response()* and *monthly_response()* functions, the highest calculated absolute correlation coefficient was targeted for the daily and monthly approach and the optimal time window was defined, which can be described with onset DOY, end DOY and the difference between the two, i.e. the length of identified time window in days. To enable useful comparison with the daily approach, the identified optimal time window for monthly data is described in DOYs. For example, if the highest calculated monthly correlation coefficient was calculated for the combination of the months June–July, the onset DOY was 152 (June 1st), the end was DOY 212 (July 31st) and the window length was 61 days.

2.4. Data analysis

All analyses were performed using R software (R Core Team, 2019). The highest calculated correlations and their respective time windows from *daily_response()* and *monthly_response()* were first compared, and the differences between the two were analysed for all proxies together and also separately for different types of proxies. To further evaluate the calculated correlations and assess the significance of the differences between the daily and monthly approach, bootstrapped correlations with 1000 bootstrapped replicates were calculated. Bootstrapping of correlations inside *daily_response()* is computationally expensive and time consuming;

therefore, it was done on a subsample of 69.4% of randomly selected chronologies.

The meta-data of the 1860 tree-ring chronologies with calculated correlations with day-wise and month-wise aggregated climate data together with related time windows are given in [Supplementary Table S1](#). Three R scripts are available via the GitHub repository (https://github.com/jernejevsenak/analysis_european_tree-ring_network): File *analysis.R* is executable and reproduces the main results presented in this study by using [Supplementary Table S1](#). *dendroTools.R* describes the extraction of correlations calculated with day-wise and month-wise aggregated temperature and precipitation data, while *SPEI.R* describes the same procedure for SPEI data. The aggregation of water balance (D_i) into daily/monthly SPEI of various scales is not possible inside the *daily_response()*/*monthly_response()* functions due to the organizational structure of both functions. Therefore, both functions were modified and available in *SPEI.R*.

3. Results and discussion

3.1. Overview of the extended European tree-ring network

The compiled extended European tree-ring network consisted of 1860 chronologies from Europe, northern Africa and western Asia, with elevations ranging from 0 to 2450 m a.s.l. (Fig. 1). The main contributor of the data used in this study was Fritz Schweingruber, who provided 30.3% of all files. There were 42 different tree species, with *Picea abies* being the most common (445 chronologies), followed by *Pinus sylvestris* (340 chronologies), *Abies alba* (225 chronologies), *Fagus sylvatica* (120 chronologies), *Larix decidua* (113 chronologies), *Pinus nigra* (101 chronologies) and *Quercus robur* (87 chronologies). The majority of measurements were tree-ring widths (67.1%), followed by early and latewood measurements (6.8% each), maximum (5.8%) and minimum (4.7%) density, latewood percentage (2.7%), early and latewood density (1.9% each), stable carbon isotope ratio ($\delta^{13}C$) (1.8%) and stable oxygen isotope ratio ($\delta^{18}O$) (less than 1%). Conifers provided 82% of analysed chronologies, with only 18% belonging to broadleaves (Fig. 2). Of the 1860 chronologies, 624 were available as already developed and standardised chronologies, while 1236 were detrended as described in section 2.1. The mean $rbar$ of individual chronologies was 0.35, ranging from 0.10 to 0.75. The minimum number of years included in the analysis was 31, with a mean of 46 and a maximum of 67 years.

3.2. Comparison of correlations calculated with day-wise and month-wise aggregated climate data

The *daily_response()* and *monthly_response()* functions were

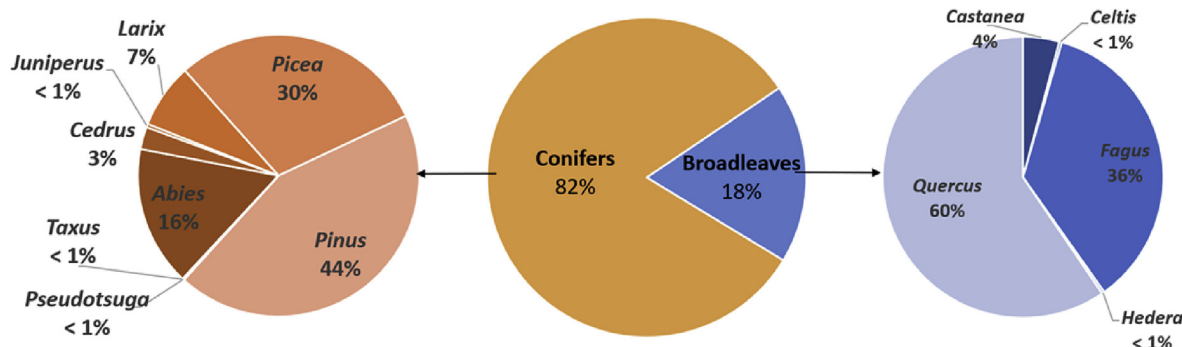


Fig. 2. Share of analysed data for conifers and broadleaves per genus.

used together with mean temperature, sum of precipitation and SPEI data on the 1860 chronologies, and the highest calculated correlation coefficients between the daily and monthly approaches were compared. While the monthly and daily approach might identify correlation coefficients from different time windows and different signs, I compared only those which had the same sign and an overlap of at least 7 days in their optimal time windows, which indicates that the correlations refer to the same climate signal. The opposite was true in about 10% of examples (10.6% for temperature, 11.0% for precipitation and 11.4% for SPEI data), which were not accounted for in further analysis.

Excluding calculations with different time windows and/or opposite positive/negative signs, the mean absolute correlation coefficient with daily temperature data was 0.467, while for monthly data, it was 0.407 (Table 1). On average, the correlation coefficient for day-wise aggregated temperature data was 0.060 higher. A greater difference was calculated for precipitation data, i.e. 0.076, for which the mean absolute daily correlation was 0.483 and mean absolute monthly correlation 0.406. Similar values to precipitation data were also calculated for SPEI data, where the mean absolute daily correlation was 0.485, mean absolute monthly correlation was 0.410 and the difference between them was 0.075. The actual benefit of using data on a daily scale could be inferred from histograms of differences between the daily and monthly approach (Fig. 3). In a few rare cases, the minimum difference between absolute correlations calculated with day-wise and month-wise aggregated data was 0, while in the most extreme case it was 0.390 (SPEI data), 0.306 (temperature data) and 0.286 (precipitation data). Standard deviations of differences were 0.043

(temperature) and 0.045 (precipitation and SPEI data).

The observed pattern of a higher difference for precipitation and SPEI data was calculated for 8 different proxies, while for earlywood density and minimum density, the difference between correlations calculated with day-wise and month-wise aggregated data was higher for temperature data (Table 1). Calculated mean differences for proxies varied from 0.033 to 0.117. Both extreme differences resulted from relatively small sample sizes. Mean differences between the daily and monthly approaches are similar to those reported by Sun and Liu (2016), who compared monthly and daily (pentated) correlations for three sites from China and obtained differences of 0.04 (precipitation), 0.06 (maximum temperature) and 0.10 (maximum temperature) in favour of daily (pentated) data. There are too few comparative studies between daily and monthly approaches to be able to compare our results further. In general, standard deviations were lower for day-wise aggregated correlations (Table 1), which indicates a more consistent climate signal in individual proxies. The highest calculated correlation coefficients are related to maximum and latewood density proxies and temperature data.

The benefit of using a daily rather than monthly approach is therefore greater for precipitation and SPEI data. To investigate this phenomenon, the characteristics of temperature, precipitation and SPEI time series were considered. Since temperature data have a clear annual pattern and higher autocorrelation in comparison to precipitation and SPEI data (e.g. Amirabadizadeh et al., 2015; Breinl and Di Baldassarre, 2019), the calculated temperature correlation coefficient with time window X is more similar to the next one calculated with the time window shifted by one day ($X + 1$ or $X -$

Table 1

Number of observations (N), mean, standard deviation, minimum and maximum absolute daily and monthly correlation coefficients and the difference (diff) between them for mean temperature, sum of precipitation and SPEI data. Summary statistics are given for all proxies together as well as for different proxies separately. Calculations in which daily and monthly correlations had different signs and/or referred to different time periods are excluded.

	proxy type	N	Daily Approach				Monthly Approach				diff
			mean	std	min	max	mean	std	min	max	
Temperature	All proxies	1500	0.467	0.115	0.216	0.826	0.407	0.120	0.162	0.795	0.060
	EW Density	31	0.494	0.083	0.313	0.678	0.397	0.084	0.221	0.573	0.097
	EW Width	96	0.446	0.088	0.289	0.770	0.373	0.086	0.196	0.700	0.073
	δ13C	27	0.477	0.101	0.321	0.701	0.431	0.113	0.237	0.656	0.046
	δ18O	9	0.609	0.087	0.435	0.716	0.555	0.086	0.364	0.642	0.053
	LW Density	34	0.675	0.090	0.457	0.796	0.642	0.092	0.424	0.753	0.033
	LW Percent	41	0.545	0.098	0.378	0.826	0.453	0.088	0.267	0.735	0.092
	LW Width	103	0.469	0.103	0.293	0.756	0.408	0.106	0.230	0.715	0.061
	MAX Density	100	0.664	0.104	0.317	0.826	0.625	0.111	0.247	0.795	0.039
	MIN Density	60	0.473	0.078	0.293	0.660	0.387	0.084	0.202	0.577	0.085
	Ring Width	999	0.436	0.093	0.216	0.804	0.377	0.095	0.162	0.772	0.059
	All proxies	1500	0.483	0.099	0.250	0.802	0.406	0.106	0.159	0.735	0.076
	EW Density	22	0.474	0.063	0.387	0.636	0.385	0.083	0.272	0.594	0.089
	EW Width	107	0.455	0.085	0.269	0.661	0.374	0.090	0.163	0.597	0.081
	δ13C	33	0.518	0.110	0.338	0.704	0.462	0.127	0.260	0.668	0.056
Precipitation	δ18O	3	0.417	0.049	0.361	0.454	0.345	0.049	0.291	0.388	0.072
	LW Density	31	0.524	0.085	0.342	0.710	0.448	0.104	0.233	0.652	0.076
	LW Percent	36	0.550	0.091	0.368	0.726	0.433	0.094	0.278	0.634	0.117
	LW Width	105	0.500	0.093	0.308	0.768	0.418	0.099	0.216	0.688	0.083
	MAX Density	98	0.548	0.101	0.315	0.746	0.479	0.108	0.265	0.689	0.069
	MIN Density	70	0.537	0.104	0.343	0.802	0.461	0.105	0.264	0.721	0.076
	Ring Width	995	0.469	0.095	0.250	0.764	0.394	0.103	0.159	0.735	0.075
	All proxies	1505	0.485	0.101	0.237	0.799	0.410	0.108	0.134	0.754	0.075
	EW Density	24	0.470	0.061	0.398	0.638	0.381	0.084	0.225	0.581	0.089
	EW Width	98	0.462	0.087	0.266	0.708	0.378	0.094	0.203	0.641	0.084
	δ13C	32	0.523	0.111	0.294	0.731	0.463	0.124	0.215	0.637	0.060
	δ18O	7	0.490	0.062	0.395	0.591	0.384	0.050	0.321	0.453	0.106
	LW Density	32	0.547	0.089	0.362	0.725	0.476	0.108	0.253	0.671	0.071
	LW Percent	35	0.536	0.094	0.355	0.722	0.423	0.100	0.240	0.640	0.113
	LW Width	105	0.495	0.092	0.347	0.779	0.412	0.098	0.228	0.688	0.082
SPEI	MAX Density	96	0.573	0.105	0.340	0.761	0.509	0.110	0.272	0.701	0.063
	MIN Density	70	0.538	0.111	0.326	0.799	0.454	0.116	0.264	0.748	0.084
	Ring Width	1006	0.470	0.096	0.237	0.783	0.397	0.103	0.134	0.754	0.073

1). In contrast, precipitation and SPEI data are less autocorrelated; therefore, change in rainfall information is more rapid, and the selection of the optimal time window is of greater benefit.

I tested this hypothesis by comparing the variability of correlation coefficients for the three climate variables. To do so, the highest calculated correlation coefficient was targeted and compared with 15 previously and 15 subsequently calculated correlations. The calculations had the same time window length, but were just shifted 15 days left and right on a calendar scale. Then, the standard deviation of correlations was calculated and compared among different climate variables. Higher standard deviations of correlation coefficients were calculated for precipitation and SPEI data (Fig. 4), which indicates that the change in correlations is more rapid for precipitation and SPEI data in comparison to temperature data. In other words, for temperature data, it matters less whether the selected time window is the optimal one because shifting a few days left or right is not particularly important in terms of the value of the calculated correlation coefficient.

3.3. Comparison of bootstrapped correlation coefficients

Due to the computationally extensive procedure, bootstrapped correlation coefficients were calculated on a subset of data representing 69.4% of all chronologies. Histograms of correlation coefficients calculated with and without bootstrapping show very similar patterns (Fig. 5). Confidence intervals for the monthly and daily approach show a considerable amount of overlap (Fig. 6). To make an inference about the statistically significant differences in means between the daily and monthly approach, the rule presented by Cumming and Finch (2005) was used, where statistically significant differences between two independent groups ($p < 0.05$) can be inferred if the share of overlap for 95% confidence intervals is no more than about half the average margin of error, that is, when the proportion overlap is about 0.50 or less. The following was the case in approximately 1% of examples: 0.62% (the overlap of the daily by the monthly confidence interval) and 1.60% (the overlap of the

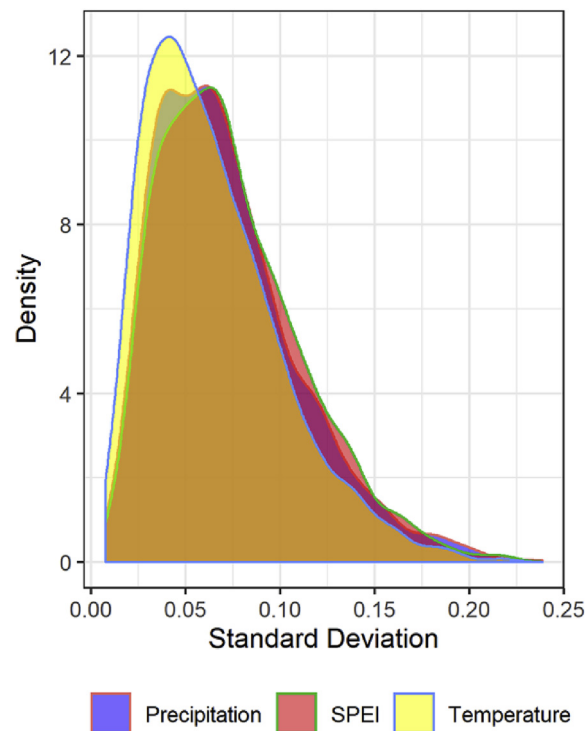


Fig. 4. Density plot of standard deviations of calculated correlation coefficients within the time window where the highest absolute value is located together with 15 previously and 15 subsequently calculated correlation coefficients.

monthly by the daily confidence interval) (Fig. 7). For more than 95% of the calculations, the confidence intervals overlap by at least 60%, which implies that just a few examples showed statistically significant differences in means between bootstrapped correlation

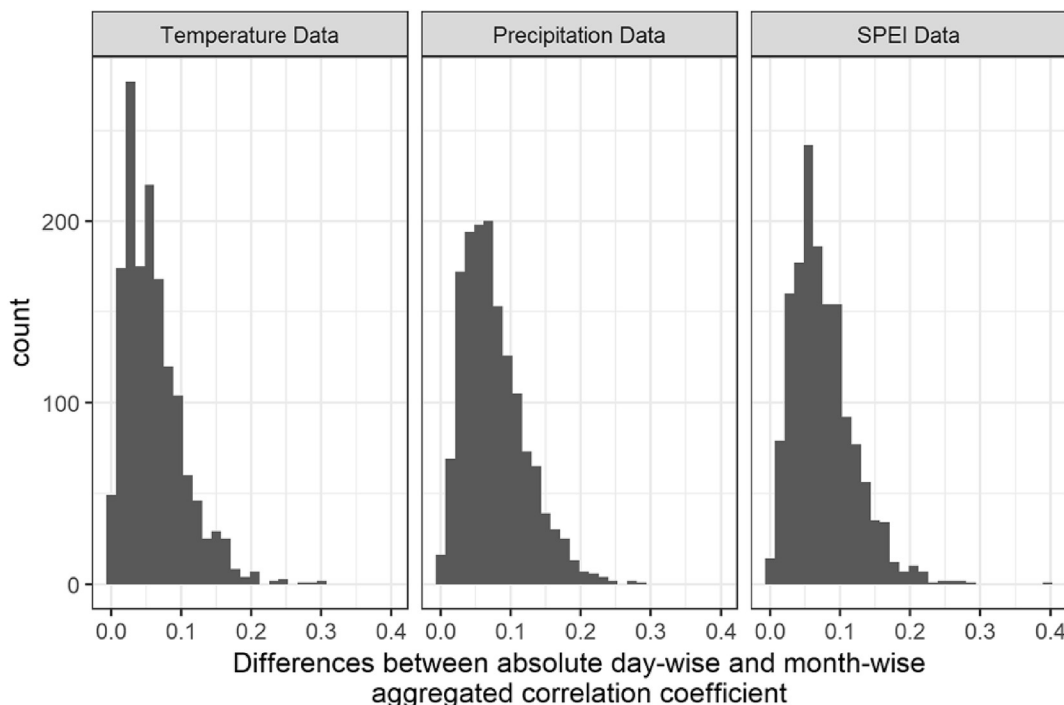


Fig. 3. Differences between absolute correlations calculated with day-wise and month-wise aggregated temperature, precipitation and SPEI data.

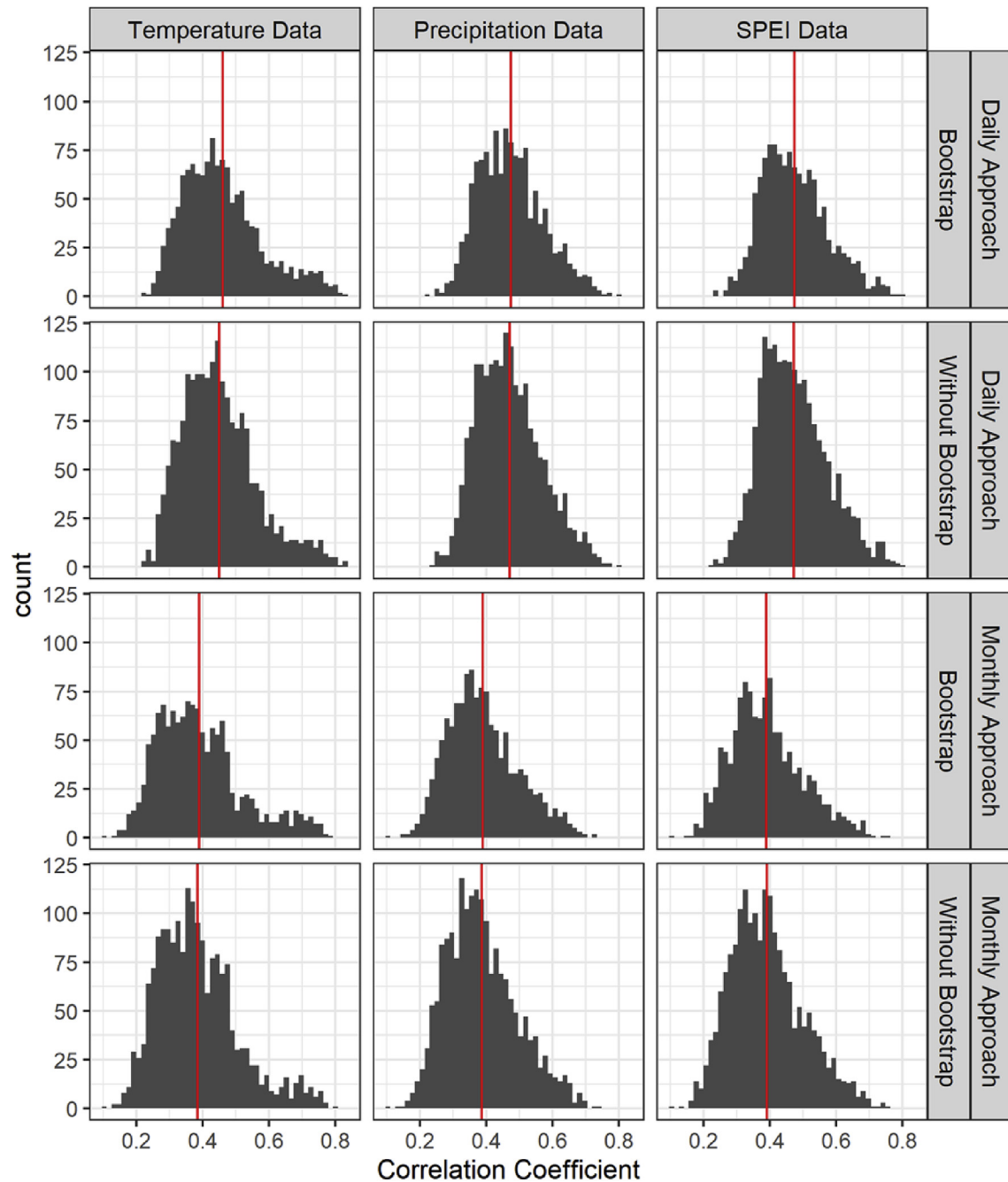


Fig. 5. Histograms of calculated absolute correlation coefficients for the daily and monthly approaches, plotted separately for the three different climate variables: Temperature, precipitation and SPEI data and two different strategies – with and without bootstrap. Red vertical lines represent the mean value of the absolute correlation coefficient for each group. (For interpretation of the references to colour in this figure legend, the reader is referred to the Web version of this article.)

coefficients resulting from day-wise and month-wise aggregated climate data.

3.4. Comparison of identified time windows from the daily and monthly approach

Each correlation coefficient analysed in section 3.2 was calculated using a specific time window, which can be described by the onset day of year (DOY), the end DOY and the difference between them, i.e. the length of identified time windows in days. To some extent, the identified time windows are related to the growing seasons and could therefore be used to characterise growing

patterns related to a specific proxy. As described in the methods section, to make a meaningful comparison between daily and monthly time windows, monthly time windows are described here in DOYs. In general, the daily approach identifies later onset and earlier ending DOY (Fig. 8, Table 2), while the biggest difference between the two approaches arises from the window lengths: daily time windows are shorter. While the median length for the daily approach was 34 (temperature), 37 (precipitation) and 35 (SPEI), the median length for the monthly approach was 61 (temperature, precipitation and SPEI data). Histograms of differences between the two approaches are centred close to zero (Fig. 9), indicating that the daily and monthly time windows differ by a small number of days.

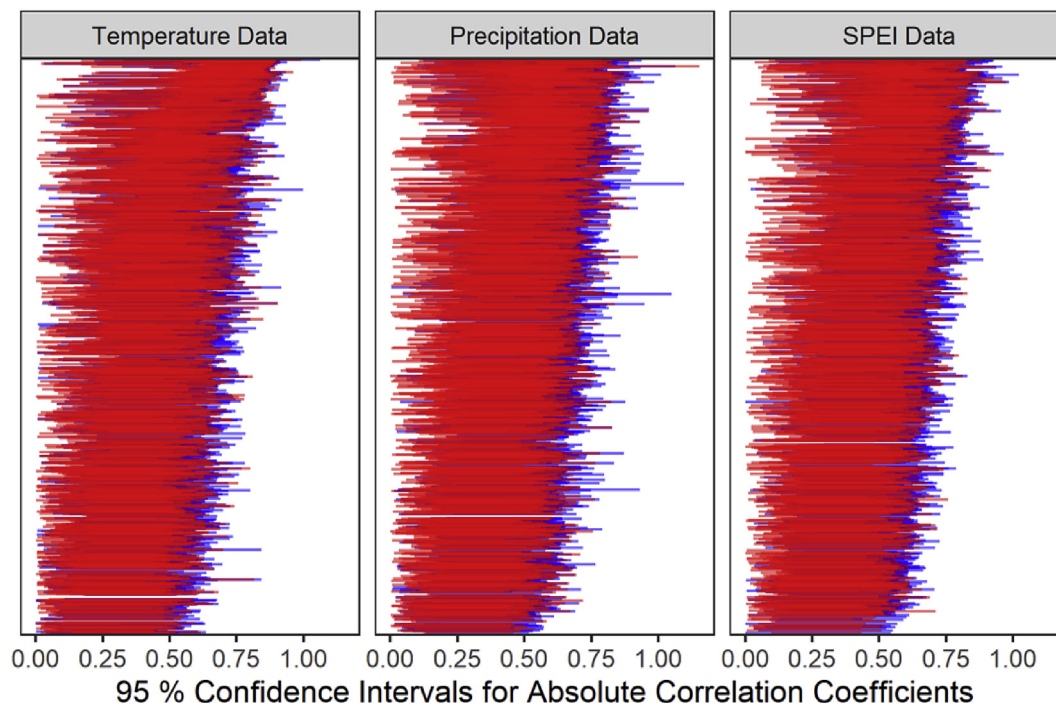


Fig. 6. Confidence intervals for bootstrapped correlations calculated with day-wise (blue) and month-wise (red) aggregated data. Only confidence intervals for correlations with equal signs and an overlap of at least 7 days are plotted. (For interpretation of the references to colour in this figure legend, the reader is referred to the Web version of this article.)

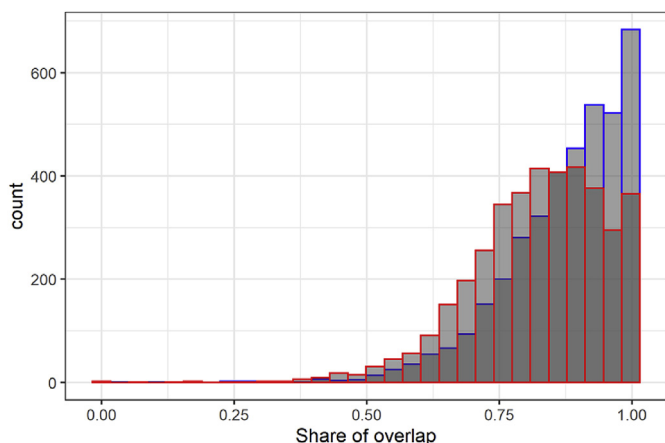


Fig. 7. Overlap of 95% confidence intervals for bootstrapped correlations calculated with day-wise and month-wise climate data. The blue colour depicts the share of overlap of the daily by the monthly confidence interval, while the red colour depicts the share of the overlap of the monthly by the daily confidence interval. (For interpretation of the references to colour in this figure legend, the reader is referred to the Web version of this article.)

In some rare cases, the time windows showed considerable differences.

Similar to the comparison of correlation coefficients (section 3.2), the greatest differences in time window characteristics for the daily and monthly approaches were calculated for SPEI and precipitation data, while temperature data showed smaller differences between the two approaches (Table 3). I assume this pattern is also related to the autocorrelation present in time series of the three climate variables (see section 3.2).

3.5. Potential applications for climate-growth relationship investigations

Further dendroclimatological applications of applying climate data on a daily scale are discussed in this section. The function *daily_response()* uses flexible time windows and removes the limits defined by calendar months and therefore results in higher calculated correlation coefficients. In addition to analysis with simple and bootstrapped correlation coefficients, which was the focus in this study, the dendroTools R package also enables the calculation of partial correlations and multiproxy analysis, where instead of calculating correlations, linear or nonlinear models are fitted and afterwards (adjusted) explained variances are extracted. In this study, correlations were calculated using the Pearson method, while *daily_response()* also allows for calculations of correlations using the Spearman and Kendall methods. Finally, there are several functions available for the interpretation of calculated correlations, including plotting and summary methods, which were recently added to the dendroTools R package.

One of the great benefits of applying climate data on a daily scale is the ability to study the changes in identified time windows over time. To illustrate this feature, I performed an additional experiment in which only tree-ring width chronologies with at least 60 years of data in the period 1950–2015 were included. Fifty-five chronologies were split into two periods, i.e. early (1950–1980) and late (1981–2010 or the most recent year), and analysed with the *daily_response()* function, where mean daily temperatures were used as the climate variable. Identified time windows were then plotted separately for early and later periods (Fig. 10). Thirty-eight out of 55 (69%) chronologies showed a shift in their time windows towards earlier DOYs, which might be related to changes in growing patterns. Those patterns could be investigated on a greater spatial scale, separately for different tree species and elevational transects. Studying climate-growth relationships on daily scales therefore opens many new possibilities. In addition to studying

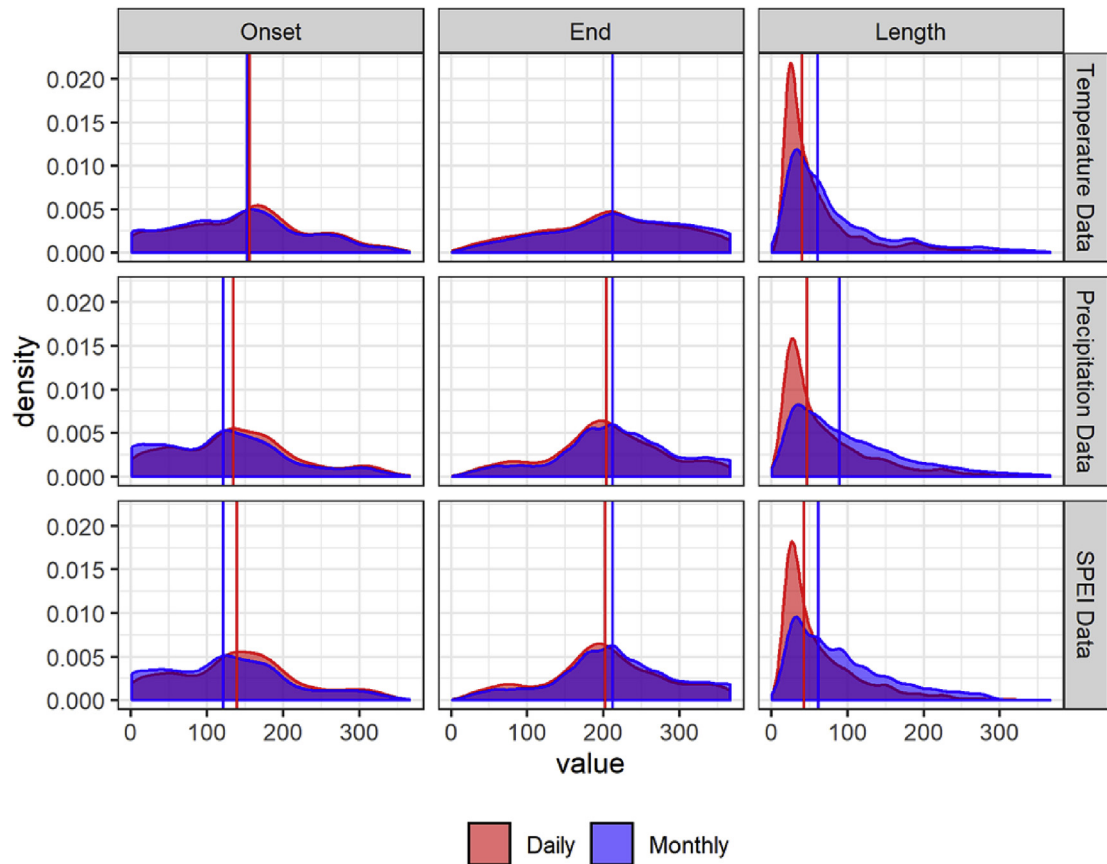


Fig. 8. Density plots for onset DOY, end DOY and time window lengths of all proxies plotted together for temperature, precipitation and SPEI data. Vertical lines depict medians.

Table 2

Median Onset DOY, End DOY and the length of optimal time windows in days, for daily and monthly approaches, separately for temperature, precipitation and SPEI data and different tree-ring proxies. Describing dates in brackets, given for Onset and End DOY, refer to a non-leap year.

		Temperature Data			Precipitation Data			SPEI Data		
		Onset DOY	End DOY	Window Length	Onset DOY	End DOY	Window Length	Onset DOY	End DOY	Window Length
Earlywood Density	Daily	142 (May 22)	175 (Jun 24)	27	65 (Mar 06)	142 (May 22)	29	99 (Apr 09)	166 (Jun 15)	33
	Monthly	91 (Apr 01)	151 (May 31)	61	32 (Feb 01)	151 (May 31)	59	32 (Feb 01)	181 (Jun 30)	59
Earlywood Width	Daily	156 (Jun 05)	197 (Jul 16)	31	125 (May 05)	179 (Jun 28)	36	149 (May 29)	189 (Jul 08)	30
	Monthly	152 (Jun 01)	212 (Jul 31)	61	121 (May 01)	212 (Jul 31)	61	121 (May 01)	212 (Jul 31)	61
$\delta^{13}\text{C}$	Daily	158 (Jun 07)	229 (Aug 17)	32	137 (May 17)	234 (Aug 22)	58	149 (May 29)	223 (Aug 11)	56
	Monthly	152 (Jun 01)	243 (Aug 31)	62	106 (Apr 16)	258 (Sep 15)	153	91 (Apr 01)	273 (Sep 30)	184
$\delta^{18}\text{O}$	Daily	106 (Apr 16)	144 (May 24)	33	134 (May 14)	161 (Jun 10)	32	94 (Apr 04)	133 (May 13)	40
	Monthly	60 (Mar 01)	151 (May 31)	151	91 (Apr 01)	212 (Jul 31)	31	91 (Apr 01)	181 (Jun 30)	61
Latewood Density	Daily	136 (May 16)	270 (Sep 27)	89	179 (Jun 28)	242 (Aug 30)	50	177 (Jun 26)	262 (Sep 19)	64
	Monthly	121 (May 01)	273 (Sep 30)	92	182 (Jul 01)	273 (Sep 30)	92	182 (Jul 01)	273 (Sep 30)	92
Latewood Percent	Daily	160 (Jun 09)	196 (Jul 15)	27	169 (Jun 18)	217 (Aug 05)	27	191 (Jul 10)	217 (Aug 05)	27
	Monthly	152 (Jun 01)	212 (Jul 31)	31	91 (Apr 01)	212 (Jul 31)	61	121 (May 01)	212 (Jul 31)	59
Latewood Width	Daily	168 (Jun 17)	213 (Aug 01)	34	156 (Jun 05)	221 (Aug 09)	34	164 (Jun 13)	211 (Jul 30)	34
	Monthly	152 (Jun 01)	212 (Jul 31)	31	152 (Jun 01)	212 (Jul 31)	61	152 (Jun 01)	212 (Jul 31)	61
Maximum Density	Daily	185 (Jul 04)	262 (Sep 19)	71	179 (Jun 28)	250 (Sep 07)	56	180 (Jun 29)	256 (Sep 13)	57
	Monthly	182 (Jul 01)	273 (Sep 30)	92	182 (Jul 01)	273 (Sep 30)	90	182 (Jul 01)	273 (Sep 30)	92
Minimum Density	Daily	148 (May 28)	194 (Jul 13)	26	92 (Apr 02)	175 (Jun 24)	51	114 (Apr 24)	175 (Jun 24)	38
	Monthly	121 (May 01)	181 (Jun 30)	61	60 (Mar 01)	181 (Jun 30)	92	60 (Mar 01)	181 (Jun 30)	91
Ring Width	Daily	154 (Jun 03)	203 (Jul 22)	33	135 (May 15)	199 (Jul 18)	36	137 (May 17)	195 (Jul 14)	35
	Monthly	152 (Jun 01)	212 (Jul 31)	61	121 (May 01)	212 (Jul 31)	61	121 (May 01)	212 (Jul 31)	61

changes in time windows over time, it would be interesting to investigate the dependences between time windows and periods of the highest rate of xylem cell production. Finally, the approach from the *daily_response()* could be used in various ecophysiological or climate reconstruction models, where higher explained variance is

expected. Following the results presented in section 3.2, the daily approach on average improves the explained variance by 5.16% (temperature data), 6.65% (precipitation data) and 6.60% (SPEI data). Examples of climate reconstructions using day-wise aggregated climate data in combination with linear and nonlinear

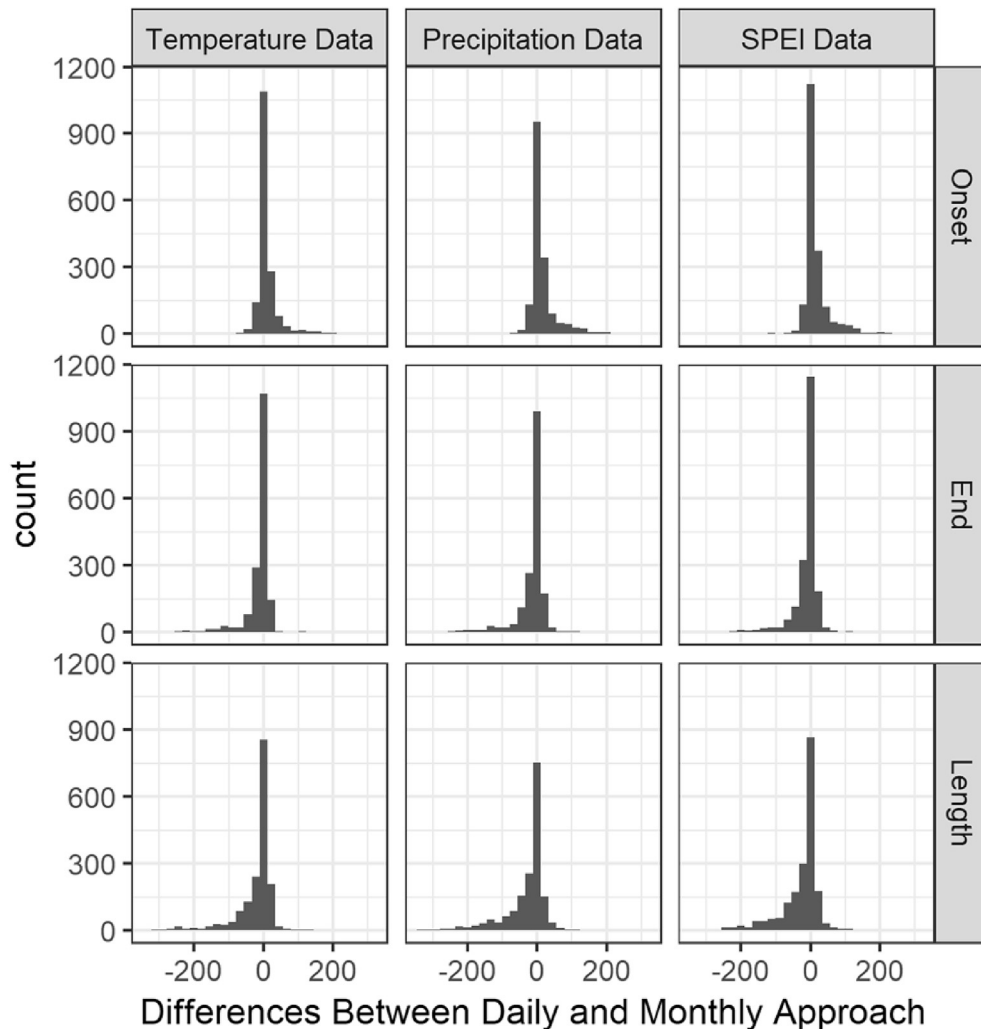


Fig. 9. Differences between the characteristics (Onset, End, Length) of identified time windows from the daily and monthly approach, calculated as daily minus monthly, plotted separately for temperature, precipitation and SPEI data.

Table 3

Summary statistics of differences between the characteristics (Onset, End, Length) of identified time windows from the daily and monthly approach, calculated as daily minus monthly, shown separately for temperature, precipitation and SPEI data.

Climate variable	Window	median	std	max	min
Temperature	Onset	3	31.3	253	−169
	End	−4	38.3	107	−331
	Length	−8	55.2	183	−344
Precipitation	Onset	5	38.4	303	−165
	End	−4	42.5	184	−317
	Length	−9	63.0	247	−344
SPEI	Onset	6	35.5	254	−165
	End	−4	36.0	108	−253
	Length	−9	53.6	187	−254

transfer functions are provided in vignettes of the *daily_response()* function on CRAN (https://cran.r-project.org/package=dendroTools/vignettes/Examples_daily_response.html).

4. Conclusions

The results presented here highlight the advantages of using day-wise aggregated climate data instead of a month-wise

approach. In comparison to correlations with month-wise aggregated climate data, correlations with day-wise aggregated climate data were on average higher by 0.060 (temperature data), 0.076 (precipitation data) and 0.075 (SPEI data). The benefit of using daily data is greater for precipitation and SPEI data, while more auto-correlated temperature series show smaller differences to the monthly approach. The results are consistent for calculations with and without bootstrapping. Based on the share of overlapped confidence intervals for bootstrapped correlations, I concluded that, except for 1% of the calculations, there are no significant differences in means between day-wise and month-wise aggregated correlation coefficients.

In this analysis, I compared only correlations which had the same sign and showed at least 7 days of overlap of their optimal time windows. I highlighted only the highest calculated correlation coefficient resulting from the *daily_response()* and *monthly_response()* functions, while potential secondary climate effects with lower correlation coefficients were not considered in this study. However, all calculated correlations are saved in a matrix and given as the first element of the function's output (Jevšenak and Levanič, 2018) so that potential users can explore those matrices and select different time windows, if needed. Furthermore, the effects of previous growing seasons are ignored solely because of

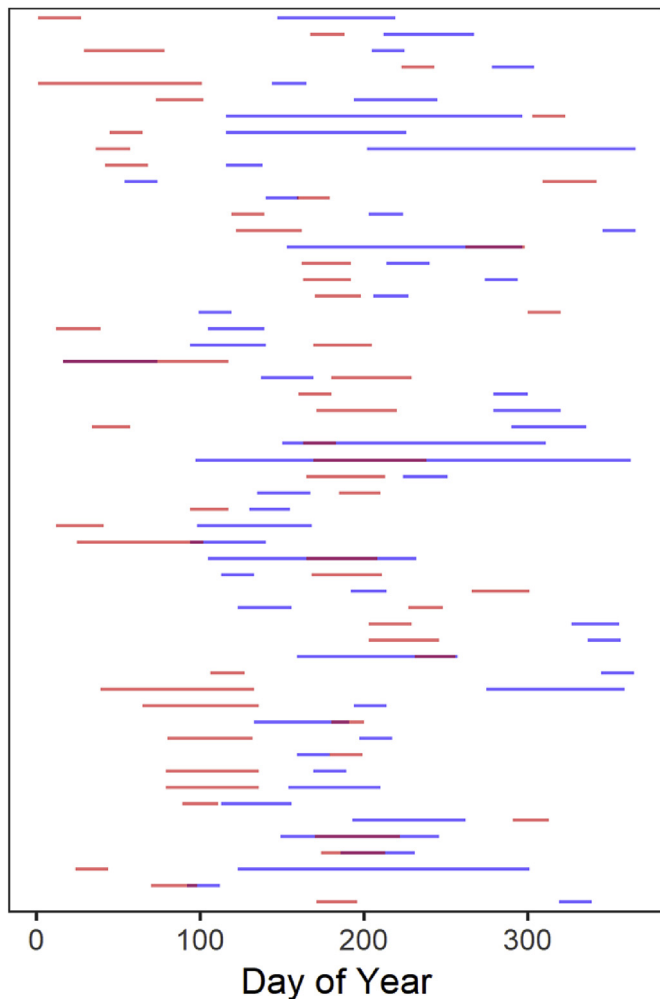


Fig. 10. Identified time windows calculated with the *daily_response()* function for early (blue colour) and late (red colour) periods. (For interpretation of the references to colour in this figure legend, the reader is referred to the Web version of this article.)

computational reasons. Again, *daily_response()* and *monthly_response()* can also be used to analyse the effects of previous growing seasons. To do so, the argument *previous_year* must be set to TRUE. The significance of the differences between the daily and monthly approach were inferred from the overlap of 95% confidence intervals. Usually, this would be done with the *t*-test, but the calculation strategy from *daily_response()* and *monthly_response()* does not allow this, since only the mean bootstrapped correlation coefficient and its lower and upper confidence intervals are saved and available for comparison.

The *daily_response()* function comes with a much higher risk of a type I error. The number of calculated correlation coefficients for each chronology and climate variable was 59 685; therefore, 2984 calculations theoretically result in a type I error. For the *monthly_response()* function, the number of calculated correlation coefficients is 78, where around 4 calculations theoretically result in type I error. In addition to much higher risk of type I errors, calculations with day-wise aggregated data are time consuming, especially when bootstrapping is applied. To calculate 59 685 bootstrapped correlation coefficients with 1000 bootstrapped samples, it takes on average slightly more than 2 h, while for the monthly approach, 78 bootstrapped correlation coefficients with 1000 bootstrapped samples are calculated in around 10–13 s.

Despite the mostly nonsignificant differences in calculated

correlation coefficients, the results presented in this paper strongly encourage the tree-ring community to seriously consider the use of daily climate data rather than the monthly data typically used in dendroclimatological studies.

Acknowledgments

Funding for this study was provided by the Slovene Research Agency: Program and Research Group “Forest biology, ecology and technology” P4-0107 and Basic Research Project J4-8216 “Mortality of lowland oak forests – consequence of lowering underground water or climate change?”. I am grateful to all researchers who have uploaded their tree-ring data to various online repositories. I acknowledge the E-OBS dataset from the EU-FP6 project UERRA (<http://www.uerra.eu>) and the Copernicus Climate Change Service, and the data providers in the ECA&D project (<https://www.ecad.eu>). The shapefile for Fig. 1 was downloaded from <http://www.natureearthdata.com/downloads/10m-cultural-vectors/>. Finally, many thanks go to the two anonymous reviewers who suggested many improvements and ideas presented in the final version of this paper.

Appendix A. Supplementary data

Supplementary data to this article can be found online at <https://doi.org/10.1016/j.quascirev.2019.105868>.

References

- Amirabadizadeh, M., Huang, Y.F., Lee, T.S., 2015. Recent trends in temperature and precipitation in the langat river basin, Malaysia. *Adv. Meteorol.* 2015, 16.
- Anchukaitis, K.J., Evans, M.N., Kaplan, A., Vaganov, E.A., Hughes, M.K., Grissino-Mayer, H.D., Cane, M.A., 2006. Forward modeling of regional scale tree-ring patterns in the southeastern United States and the recent influence of summer drought. *Geophys. Res. Lett.* 33.
- Babst, F., Bodesheim, P., Charney, N., Friend, A.D., Girardin, M.P., Klesse, S., Moore, D.J.P., Seftigen, K., Björklund, J., Bouriaud, O., Dawson, A., DeRose, R.J., Dietze, M.C., Eckes, A.H., Enquist, B., Frank, D.C., Mahecha, M.D., Poulter, B., Record, S., Trouet, V., Turton, R.H., Zhang, Z., Evans, M.E.K., 2018. When tree rings go global: challenges and opportunities for retro- and prospective insight. *Quat. Sci. Rev.* 197, 1–20.
- Babst, F., Bouriaud, O., Poulter, B., Trouet, V., Girardin, M.P., Frank, D.C., 2019. Twentieth century redistribution in climatic drivers of global tree growth. *Sci. Adv.* 5, eaat4313.
- Babst, F., Poulter, B., Trouet, V., Tan, K., Neuwirth, B., Wilson, R., Carrer, M., Grabner, M., Tegel, W., Levanic, T., Panayotov, M., Urbinati, C., Bouriaud, O., Ciais, P., Frank, D., 2013. Site- and species-specific responses of forest growth to climate across the European continent. *Glob. Ecol. Biogeogr.* 22, 706–717.
- Beck, W., Sanders, T.G.M., Pofahl, U., 2013. CLIMTREG: detecting temporal changes in climate–growth reactions – a computer program using intra-annual daily and yearly moving time intervals of variable width. *Dendrochronologia* 31, 232–241.
- Becker, G., 2012. SearchTrees: Spatial Search Trees. R package, version 0.5.2. <https://CRAN.R-project.org/package=SearchTrees>.
- Beguier, S., Vicente-Serrano, S.M., 2017. SPEI: Calculation of the Standardised Precipitation–Evapotranspiration Index. R package, version 1.7. <https://CRAN.R-project.org/package=SPEI>.
- Bhuyan, U., Zang, C., Menzel, A., 2017. Different responses of multispecies tree ring growth to various drought indices across Europe. *Dendrochronologia* 44, 1–8.
- Breidl, K., Di Baldassarre, G., 2019. Space-time disaggregation of precipitation and temperature across different climates and spatial scales. *J. Hydrol.: Reg. Stud.* 21, 126–146.
- Breitenmoser, P., Brönnimann, S., Frank, D., 2014. Forward modelling of tree-ring width and comparison with a global network of tree-ring chronologies. *Clim. Past* 10, 437–449.
- Bunn, A.G., 2008. A dendrochronology program library in R (dplR). *Dendrochronologia* 26, 115–124.
- Cailleret, M., Jansen, S., Robert, E.M.R., Desoto, L., Aakala, T., Antos, J.A., Beikircher, B., Bigler, C., Bugmann, H., Caccianiga, M., Cada, V., Camarero, J.J., Cherubini, P., Cochard, H., Coyea, M.R., Cufar, K., Das, A.J., Davi, H., Delzon, S., Dorman, M., Gea-Izquierdo, G., Gillner, S., Haavik, L.J., Hartmann, H., Heres, A.-M., Hultine, K.R., Janda, P., Kane, J.M., Kharuk, V.I., Kitzberger, T., Klein, T., Kramer, K., Lens, F., Levanic, T., Linares Calderon, J.C., Lloret, F., Lobo-Do-Vale, R., Lombardi, F., López Rodríguez, R., Mäkinen, H., Mayr, S., Mészáros, I., Metsaranta, J.M., Minunno, F., Oberhuber, W., Papadopoulos, A., Peltoniemi, M., Petritan, A.M., Rohner, B., Sangüesa-Barreda, G., Sarris, D., Smith, J.M., Stan, A.B.,

- Sterck, F., Stojanović, D.B., Suarez, M.L., Svoboda, M., Tognetti, R., Torres-Ruiz, J.M., Trotsiuk, V., Villalba, R., Vodde, F., Westwood, A.R., Wyckoff, P.H., Zafirov, N., Martínez-Vilalta, J., 2017. A synthesis of radial growth patterns preceding tree mortality. *Glob. Chang. Biol.* 23, 1675–1690.
- Castagneri, D., Petit, G., Carrer, M., 2015. Divergent climate response on hydraulic-related xylem anatomical traits of *Picea abies* along a 900-m altitudinal gradient. *Tree Physiol.* 35, 1378–1387.
- Cook, E.R., Kairiukstis, L.A., 1992. *Methods of Dendrochronology: Applications in the Environmental Sciences*. Kluwer Academic Publishers, Dordrecht.
- Cornes, R.C., van der Schrier, G., van den Besselaar, E.J.M., Jones, P.D., 2018. An ensemble version of the E-OBS temperature and precipitation data sets. *Geophys. Res. Lett.*: Atmosphere 123, 9391–9409.
- Cumming, G., Finch, S., 2005. Inference by eye: confidence intervals and how to read pictures of data. *Am. Psychol.* 60, 170–180.
- Danis, P.A., Hatté, C., Misson, L., Guiot, J., 2012. MAIDENiso: a multiproxy biophysical model of tree-ring width and oxygen and carbon isotopes. *Can. J. For. Res.* 42, 1697–1713.
- Grissino-Mayer, H.D., Fritts, H.C., 1997. The International Tree-Ring Data Bank: an enhanced global database serving the global scientific community. *Holocene* 7, 235–238.
- Hacket-Pain, A.J., Ascoli, D., Vacchiano, G., Biondi, F., Cavin, L., Conedera, M., Drobyshev, I., Liñán, I.D., Friend, A.D., Grabner, M., Hartl, C., Kreyling, J., Lebourgeois, F., Levanič, T., Menzel, A., van der Maaten, E., van der Maaten-Theunissen, M., Muffler, L., Motta, R., Roibu, C.-C., Popa, I., Scharnweber, T., Weigel, R., Wilmking, M., Zang, C.S., 2018. Climatically controlled reproduction drives interannual growth variability in a temperate tree species. *Ecol. Lett.* 21, 1833–1844.
- Hargreaves, G.H., Samani, Z., 1985. Reference crop evapotranspiration from temperature. *Appl. Eng. Agric.* 1, 96–99.
- Hofstra, N., Haylock, M., New, M., Jones, P.D., 2009. Testing E-OBS European high-resolution gridded data set of daily precipitation and surface temperature. *Geophys. Res. Lett.*: Atmosphere 114.
- Jevšenak, J., Levanič, T., 2018. *dendroTools*: R package for studying linear and nonlinear responses between tree-rings and daily environmental data. *Dendrochronologia* 48, 32–39.
- Land, A., Remmele, S., Schönbein, J., Küppers, M., Zimmermann, R., 2017. Climate-growth analysis using long-term daily-resolved station records with focus on the effect of heavy precipitation events. *Dendrochronologia* 45, 156–164.
- Liang, W., Heinrich, I., Simard, S., Helle, G., Liñán, I.D., Heinken, T., 2013. Climate signals derived from cell anatomy of Scots pine in NE Germany. *Tree Physiol.* 33, 833–844.
- Linderholm, H.W., 2006. Growing season changes in the last century. *Agric. For. Meteorol.* 137, 1–14.
- Loehle, C., 2009. A mathematical analysis of the divergence problem in dendroclimatology. *Clim. Change* 94, 233–245.
- Pritzkow, C., Wazny, T., Heuvsner, K.U., Słowiński, M., Bieber, A., Liñán, I.D., Helle, G., Heinrich, I., 2016. Minimum winter temperature reconstruction from average earlywood vessel area of European oak (*Quercus robur*) in N-Poland. *Palaeogeogr. Palaeoclimatol. Palaeoecol.* 449, 520–530.
- R Core Team, 2019. R: A Language and Environment for Statistical Computing (Vienna, Austria).
- Sánchez-Salguero, R., Camarero, J.J., Carrer, M., Gutiérrez, E., Alla, A.Q., Andreu-Hayles, L., Hevia, A., Koutavas, A., Martínez-Sancho, E., Nola, P., Papadopoulos, A., Pasho, E., Toromani, E., Carreira, J.A., Linares, J.C., 2017. Climate extremes and predicted warming threaten Mediterranean Holocene firs forests refugia. *Proc. Natl. Acad. Sci. U.S.A.* 114, E10142–E10150.
- Sánchez-Salguero, R., Camarero, J.J., Rozas, V., Génova, M., Olano, J.M., Arzac, A., Gazol, A., Caminero, L., Tejedor, E., de Luis, M., Linares, J.C., 2018. Resist, recover or both? Growth plasticity in response to drought is geographically structured and linked to intraspecific variability in *Pinus pinaster*. *J. Biogeogr.* 45, 1126–1139.
- Sanders, T., Pitman, R., Broadmeadow, M., 2014. Species-specific climate response of oaks (*Quercus* spp.) under identical environmental conditions. *iForest* 7, 61–69.
- Schönbein, J., Land, A., Friedrich, M., Glaser, R., Küppers, M., 2015. Seasonal reconstruction of summer precipitation variability and dating of flood events for the millennium between 3250 and 2250 Years BC for the Main Region, southern Germany. In: Schulz, M., Paul, A. (Eds.), *Integrated Analysis of Interglacial Climate Dynamics (INTERDYNAMIC)*. Springer International Publishing, Cham, pp. 127–131.
- Shishov, V.V., Tychkov, I.I., Popkova, M.I., Ilyin, V.A., Bryukhanova, M.V., Kiryanov, A.V., 2016. VS-oscilloscope: a new tool to parameterize tree radial growth based on climate conditions. *Dendrochronologia* 39, 42–50.
- St. George, S., 2014. An overview of tree-ring width records across the Northern Hemisphere. *Quat. Sci. Rev.* 95, 132–150.
- Sun, C., Liu, Y., 2016. Climate response of tree radial growth at different timescales in the qinling mountains. *PLoS One* 11, e0160938.
- Tejedor, E., Saz, M.A., Esper, J., Cuadrat, J.M., de Luis, M., 2017. Summer drought reconstruction in northeastern Spain inferred from a tree ring latewood network since 1734. *Geophys. Res. Lett.* 44, 8492–8500.
- Vicente-Serrano, S.M., Beguería, S., López-Moreno, J.I., 2010. A multiscalar drought index sensitive to global warming: the standardized precipitation evapotranspiration index. *J. Clim.* 23, 1696–1718.
- Wang, Q., Shi, P., Lei, T., Geng, G., Liu, J., Mo, X., Li, X., Zhou, H., Wu, J., 2015. The alleviating trend of drought in the Huang-Huai-Hai Plain of China based on the daily SPEI. *Int. J. Climatol.* 35, 3760–3769.
- Yin, H., Donat, M.G., Alexander, L.V., Sun, Y., 2015. Multi-dataset comparison of gridded observed temperature and precipitation extremes over China. *Int. J. Climatol.* 35, 2809–2827.
- Zhao, S., Pederson, N., D'Orangeville, L., HilleRisLambers, J., Boose, E., Penone, C., Bauer, B., Jiang, Y., Manzanedo, Rubén D., 2019. The International Tree-Ring Data Bank (ITRDB) revisited: data availability and global ecological representativity. *J. Biogeogr.* 46, 355–368.